DRAG-FREE CONTROL SYSTEM FOR FRAME DRAGGING MEASUREMENTS BASED ON COLD ATOM INTERFEROMETRY

Walter Fichter[1], Alexander Schleicher[2], Laszlo Szerdahelyi[1], Stephan Theil[2], Phil Airey[3]

[1] EADS Astrium, Friedrichshafen, Germany
[2] ZARM, University of Bremen, Bremen, Germany
[3] ESA/ESTEC, Noordwijk, The Netherlands

Abstract

This paper describes the design and analysis of the Drag-Free and Attitude Control System (DFACS) for frame dragging measurements using a cold atom interferometer. The general architecture of the DFACS is derived and important aspects of the control system are discussed. This includes requirements and constraints, design and equipment issues. The actual control algorithms derived in this paper are designed as decoupled SISO controllers using modern optimal control theory (LQG, H_∞). The performance of the control system is analysed in a comprehensive simulation campaign. From the results it can be concluded that the proposed system can meet the requirements for frame dragging measurements, with very little additional technology adaptation for the drag-free sensor and micro-propulsion system.

Keywords: Drag-Free Control, Lense-Thirring Effect, Micro-Propulsion, FEEP

INTRODUCTION

The "Hyper-Precision Cold Atom Interferometry in Space" (HYPER) mission will test General Relativity by mapping the spatial structure of the gravitomagnetic (Lense-Thirring) effect of the Earth with about 3-5% precision. This is done by comparing rate measurements of a cold atom interferometer (Atomic Sagnac Unit, ASU) with "inertial" attitude measurements of an extremely precise star tracker (PST) with respect to a guide star. An overview of the HYPER spacecraft design is given in references [1, 2]. The full documentation can be found under [5].

The HYPER spacecraft shall fly in a near polar sun-synchronous orbit, and the pointing direction of the precision star tracker to the guide star is approximately perpendicular to the orbit plane. Precise measurements of the ASU and PST are taken in the two axes perpendicular to the PST pointing direction.

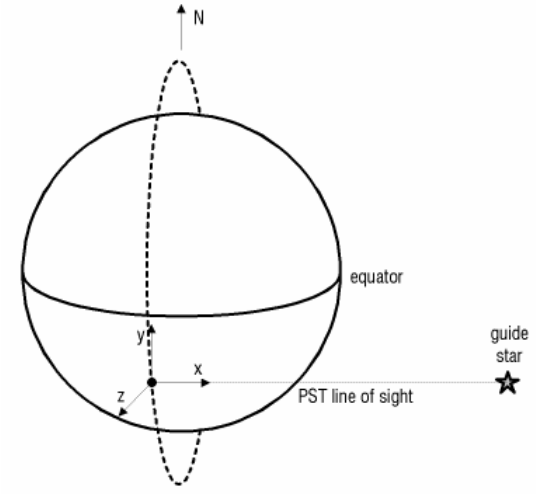

Fig 1: HYPER orientation

The operation of these two precision measurement devices (ASU, PST) places stringent requirements on the rate, attitude, and linear acceleration of the spacecraft, i.e. the drag-free and attitude control system (DFACS) has to provide a very "quiet" environment.

The DFACS requirements, design, and technological impact on sensor and actuator development is discussed in the rest of the paper.

REQUIREMENTS AND DESIGN CONSTRAINTS

Requirements

In order to obtain unambiguous phase measurements (i.e. rate measurements for science purposes) from the ASU, an operational envelope in terms of rotation rate as well as linear and angular acceleration has to be maintained by the DFACS. This envelope is defined by the performance requirements in Table 1.

Requirement	3σ-Value	1σ-Value
Acceleration at DFP (each axis)	$< 1.2 \cdot 10^{-8}$ m/s^2	$< 4 \cdot 10^{-9}$ m/s^2
Angular accelerations around transverse axes	$< 2.4 \cdot 10^{-8}$ rad/s^2	$< 8 \cdot 10^{-9}$ rad/s^2
Rate around PST bore-sight	$< 1 \cdot 10^{-6}$ rad/s	$< 3.3 \cdot 10^{-7}$ rad/s
Rigid body rate around transverse axes	$< 4.3 \cdot 10^{-8}$ rad/s	$< 1.45 \cdot 10^{-8}$ rad/s
Pointing around the transverse axes	< 0.035 arcsec	< 0.0012 arcsec
Pointing around bore-sight	< 120 arcsec	< 40 arcsec

Table 1: DFACS requirements.

In addition to the requirements induced by the ASU's operational envelope there is also a stringent requirement on the pointing accuracy of the spacecraft: in order to guarantee sufficient accuracy of the PST measurements it is crucial that the guide star remains within one pixel during the science operation leading to the required pointing accuracy of ½ pixel around the axes transverse to the boresight. The pointing accuracy around the boresight is uncritical and chosen to be close the required inertial attitude knowledge. The pointing requirements are summarized in Table 1. In the following the "transverse" axes are denoted by "Y" and "Z", the PST pointing axis (boresight, "roll") is denoted by "X".

The 3σ requirements on acceleration, angular acceleration and rotation rates have to be met in a certain frequency band only as the ASU itself has two mechanisms that attenuate and/or reject phase measurement disturbances:

1. The ASU itself acts as a low pass, since it is operated as a sampled device with a sampling ("corner") frequency of 0.3 Hz.
2. The ASU has to have a built-in phase correction mechanism that rejects low frequency disturbances. Here, low frequency means time constants of 8 h or more. This is actually the same mechanism that is required to acquire the central fringe of the measurement.

That leaves the frequency band from 8 h to 0.3 Hz in which the control system has to reject disturbances on acceleration, rate, and pointing. Thus, any signal to be evaluated has to be filtered with an appropriate band-pass filter before analyzing it (see Fig 11).

Forces and Torques

In order to have a better understanding of the environmental forces and torques to be expected during the course of the mission, worst case disturbance profiles were generated via simulation. In these simulations the seasonal variations of the environment over the year as well as the expected operational attitudes were considered using the simulation parameters shown in Table 2.

Orbit Parameters	
Inclination	99.5081 deg
Argument of perigee	90.0 deg
Semi-major axis	7384396 m
Eccentricity	$9.9928 \cdot 10^{-4}$
Right ascension of ascending node	Depends on date (sun-synchronous orbit)
SC Parameters	
SC attitude variations	±30 deg variation about Y,Z at 10 deg steps
SC moments of inertia	Ixx = 300 kg·m^2, Iyy = Izz = 250 kg·m^2
SC mass	770 kg
MSIS86 Density Model Parameters (pessimistic values)	
F10.7 (mean)	380
F10.7_prev (previous day)	380
AP (magnetic activity index)	300

Table 2: Simulation Parameters.

The worst case disturbances profiles for the total environmental forces and torques identified during these simulation runs are shown in Fig 2 and Fig 3. The contributions of each disturbance source are summarized in Table 3.

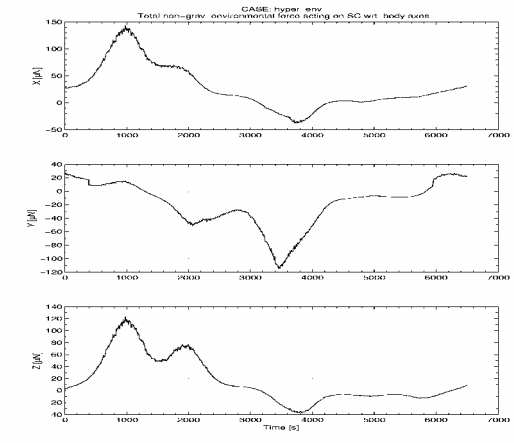

Fig 2: Total environmental force (1 orbit).

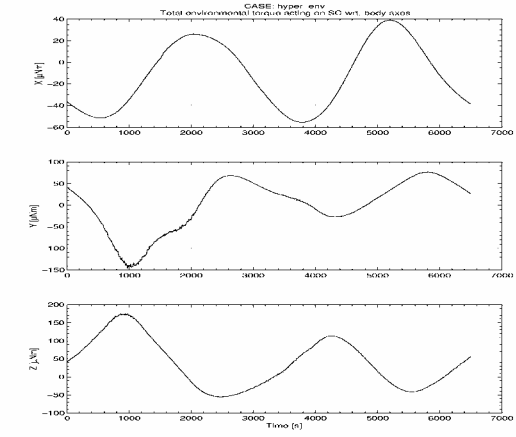

Fig 3: Total environmental torque (1 orbit).

Disturbance Forces	
Gravity gradient (DFP offset from CoM ≈ 10cm in YZ plane)	150 μN (in Y and Z)
Air drag	34 μN (average at MSIS max) 120 μN (daily peak at MSIS max)
Solar Pressure Force	15 – 20 μN
Earth IR and Albedo	4 μN (negligible)
High altitude winds	± 3.4 μN (negligible)
Thermal emission	< 2 μN (negligible)
RF emission	negligible
Disturbance Torques	
Magnetic moment (at 1 Am^2)	up to 50 μNm
Gravity gradient torque	80 μNm
Air drag induced torque	6.5 μNm (average) 100 μNm (max)
Solar pressure torque	up to 10 μNm
Thrust vector misalignment (assumption: 1.5 deg)	about 2.5 % of X-axis control torque

Table 3: Disturbance forces and torques summary.

SYSTEM DESIGN

Functional Architecture

The functional block diagram of the DFACS is shown in Fig 4. The drag-free sensors (DFS) are used to measure and control linear accelerations. Two of them are used in order to place the drag-free point close to the ASU center. Optionally one DFS can be used, however, this requires an on board gravity gradient model for placement of the drag-free point.

Attitude control is performed using the two attitude angle measurements transverse to the pointing direction of the precision star tracker (PST). The attitude measurement around the remaining "roll" axis (PST pointing axis) is performed with a conventional star tracker.

A GPS receiver together with the 3-axis star sensor is needed in order to estimate the gravity gradient on board. This is required for (ASU internal) active compensation of the gravity gradient effect.

Actuation is realized on the basis of electrical micro-propulsion (FEEP system).

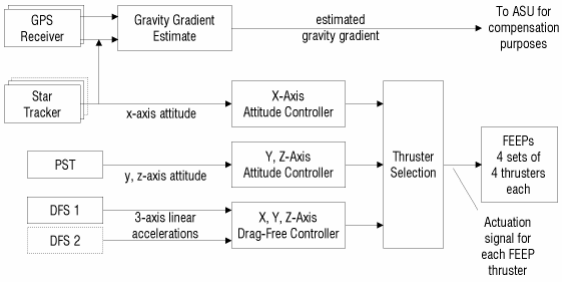

Fig 4: DFACS architecture

Sensor and Actuator Configuration

Drag-Free Sensor and Precision Star Tracker. In Fig 5 the configuration of the drag-free sensors with respect to the ASU planes and the PST boresight is shown. The connecting line between the drag-free sensors is coincident with the ASU plane intersection line. The PST boresight is parallel to this line. This leads to a configuration that is insensitive to angular accelerations around the boresight, i.e. the control loops in the "transverse" axes are decoupled from the 3-axis star sensor performance.

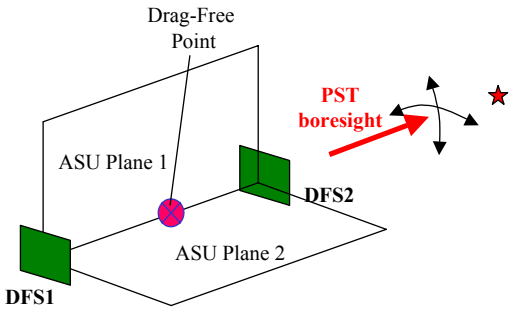

Fig 5: Drag-free sensor configuration

Thruster Configuration. The thruster configuration is shown in Fig 6. It is relatively simple and leads to a very simple thruster actuation logic. Furthermore it provides redundancy and a maximum clearance with respect to the solar arrays.

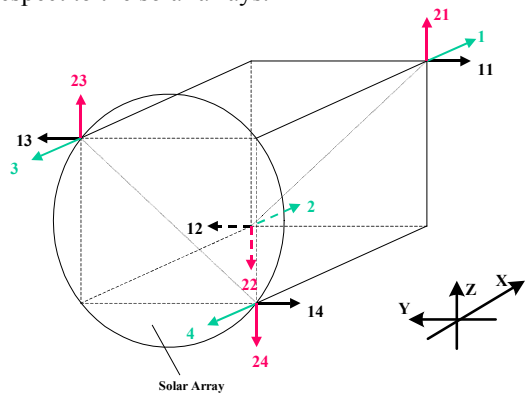

Fig 6: Thruster arrangement.

Modes and Sensor Initialization

The following DFACS modes are foreseen:

- Inertial Pointing Mode. In this mode the DFS and PST have to be initialised.
  - The DFS acquisition is driven by the gravity gradient and the maximum range is in the order of 10^{-6} m/s^2.
  - The misalignment between 3-axis star tracker and PST is about 50 arcsec. The PST field of view is ±25 arcsec. Thus, a scan strategy for the guide star is necessary.

  The inertial pointing mode includes also re-orientation maneuvers.

- Science Mode. In this modes science measurements are taken.
  - Hold Mode. Control with respect to star spot at initialisation.
  - Control Mode. Control star spot at zero position and keep it there.

The duration of a re-orientation maneuver is composed of

1. time needed for the slew maneuver itself and
2. settling time to achieve steady state conditions.

The time for the slew maneuver itself is plotted in Fig 7. A typical 30 deg slew takes about 0.37 h. As a conservative estimation, the total maneuver including settling takes typically less than one hour.

The maximum rate and acceleration during the maneuver is $4.5 \cdot 10^{-4}$ rad/s and $2.9 \cdot 10^{-7}$ rad/s^2, respectively. This means that both, drag-free sensor and 3-axis star tracker can remain switched on/ operational during the slew.

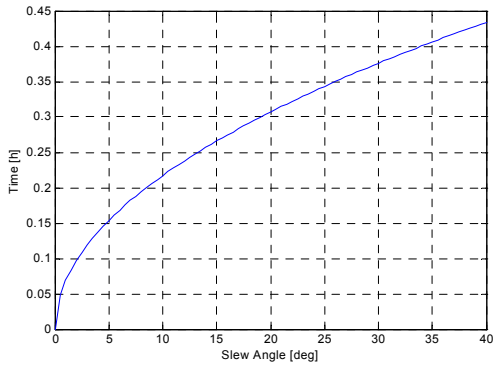

Fig 7: Slew time as a function of slew angle.

FEEDBACK CONTROL

Based on the general structure of the DFACS that has been derived earlier, the different controller algorithms are derived. As the spacecraft will experience only small deviations from the set point the individual control channels for the attitude and the drag-free control are separated leading to a set of controllers that are derived using simple one dimensional models. The validity of the approach will be verified by the simulations.

Attitude Controller

The three attitude controllers are derived using LQG theory which has been successfully applied to similar drag-free control problems. The attitude controllers shall use angle information only, i.e. the

attitude around the Y and the Z axis shall be controlled with the attitude information from the precision star tracker (PST) and the attitude around the X axis shall use the attitude measurements from the additional 3-axis star tracker. All three controllers are designed as discrete LQG controllers using a simple double integrator plant $1/s^2$. The standard LQG controllers are modified to include a model of the dominant disturbances for each axis in order to achieve the necessary disturbance rejection.

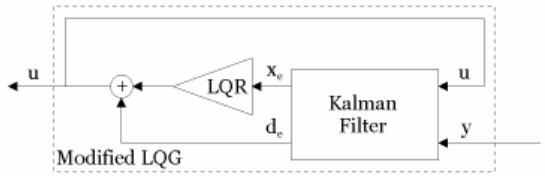

Fig 8: Modified LQG with disturbance estimation

The dominant disturbance is assumed to be sinusoidal with a frequency of roughly two times the orbit frequency. The augmented control variable then is

$$u = -K \cdot x_e - d_e$$

All of the resulting attitude controllers are in discrete time with a sampling frequency of 10 Hz.

As an alternative a second set of attitude controllers for the Y and Z axis is derived that uses additional angular acceleration information that is derived from the linear acceleration information of the DFS (only possible for the configuration with 2 DFS).

Drag-Free Controller

The three drag-free controllers are derived using H_∞-theory. The application of robust closed-loop shaping techniques is especially well suited for the design of drag-free controllers since the requirements are usually specified in a specific frequency region which are easily translated into requirements on the sensitivity functions of the closed-loop system.

The weighting scheme chosen for the design is the standard mixed-sensitivity approach with weights on the sensitivity S_y (weight W_e) and the complementary sensitivity T_y (weight W_y). The sensitivity functions of the resulting closed-loop systems are shown in Fig 9.

Under the assumption that the accelerometer dynamics are very fast compared to the drag-free control closed-loop dynamics, the plant will be unity.

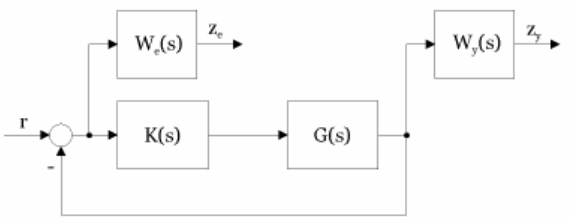

Fig 9: Mixed-sensitivity approach

The derived controllers are continuous and are then discretized with a sampling frequency of 10 Hz.

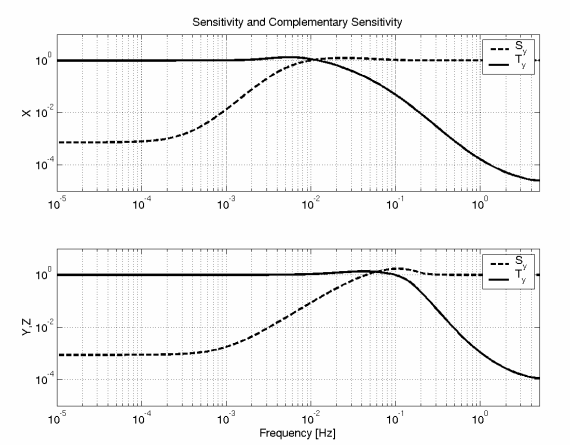

Fig 10: Closed-loop sensitivity functions

The drag-free controllers derived here are used for both drag-free sensor configurations (two DFS or one DFS in combination with gravity gradient estimation).

SIMULATION

Simulation Setup

Purpose. A detailed simulation model of the DFACS of HYPER was established in Matlab/Simulink in order to

- validate drag-free and attitude control concept and algorithms
- confirm the normal distribution nature of the PST measurement signal
- assess different measurement concepts

- validate PST acquisition and assess its entry conditions, initial rate and attitude errors

Models. The simulation model is structured in the following main components: Environment, actuators, sensors, controller and spacecraft orbit and attitude dynamics model. In addition to the environmental effects such as gravitational influences from earth, sun and moon, atmospheric drag forces and torques, magnetic disturbance torque, solar radiation forces and torques, Albedo radiation forces and torques, gravity gradient torque and eclipse model, the environmental model computed the gravity gradient accelerations at the spacecraft center of mass as well, which is necessary for the calculation of the measured accelerations at the DFS position.

The actuator subsystem model contains 12 individual FEEP units. The sensor subsystem model is composed of the precision star tracker model, a 3-axis star tracker model, 2 drag-free sensor models and a GPS receiver model. The GPS receiver model provides spacecraft position measurements. This is necessary when only one DFS is used in combination with an on board earth gravity gradient model for linear acceleration measurements (drag-free point within the ASU instrument).

The controller model is divided into 4 different parts including measurement data processing, mode control, control algorithms and control command computation. The mode control implements 3 modes: stand-by, hold, and control mode. The hold mode is entered after activation of the DFACS and the control system damps the rates on all spacecraft axes during this mode. The reference attitude is the instantaneous attitude at the activation of the controller in hold mode thereby reducing the initial response of the high-bandwidth attitude controller. Note that the drag-free controller is inactive during hold mode. The control mode follows the hold mode when the hold mode converges successfully. The initial phase of the control mode performs a transition phase where the attitude reference is smoothly changed until the desired attitude is reached. The drag-free controller is also in operation in this mode.

Simulation Campaign. The simulation campaign was divided into 3 parts (I) acquisition of PST, i.e. assessment of initial rate and attitude errors that the attitude controller can accommodate, (II) assess and validate the drag-free controller employing 2 DFS sensors under different test objectives (the baseline design) and (III) assess and validate the drag-free controller using only one DFS sensor in combination with an on-board gravity-gradient model (optional design).

For (I) all possible combinations of initial attitude errors of [0, 15] arcsec for both PST Y and Z axes and initial rate errors of [0, 1, 2, 3] arcsec/sec for all spacecraft axes were simulated.

The test objectives for (II) incorporated the variation of various parameters one at a time such as spacecraft mass and moments of inertia, spacecraft magnetic moment, drag-free point distance from spacecraft's centre of mass, introduction of coupling between drag-free and attitude control by means of thrust mismatch, variation of DFS bias, different guide star selections as well as different season selections in order to experience eclipse. This resulted in about 20 different sets of test cases for (II).

For (III) only a subset of these simulation cases were performed.

In summary, simulation cases of type (I) assess the acquisition performance whereas simulation cases of type (II) and (III) constitute the steady-state performance analysis of the DFACS.

In order to take into account the filtering effect of the ASU phase control mechanism and the ASU sampling effect, the simulated data was post processed with a band-pass with the frequency characteristics shown in Fig 11.

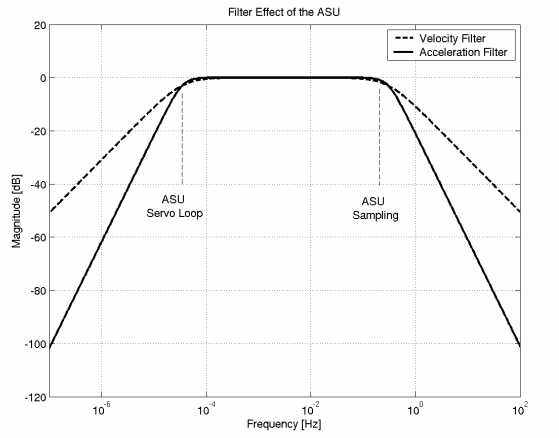

Fig 11: Filter effect of the ASU.

Results

The results of the steady state performance analysis for the baseline design (two DFS) and the optional design (one DFS) are summarised in Table 4 together with the performance requirements. It can be seen that most requirements are met with the following two exceptions:

1) For the optional control system with one DFS the acceleration slightly exceeds the requirement however, at this stage this is not considered to be problematic.
2) The angular rate around the Y and Z axis exceeds the requirement. The reason is the angular motion that is caused by controlling the guide star to be in the center of the PST's central pixel, i.e. not considering/ compensating any aberration effect caused by the spacecraft orbital motion. It should be kept in mind that this strategy is necessary for sufficient accurate PST measurements (error distribution). A time history is shown in Fig 15, which shows the "deterministic" effect in the Y and Z rates.

Since the original rate requirement specification is derived such that it corresponds to 1/10 of the central fringe, it might be possible to re-specify this parameter with a somewhat relaxed number say, 30% more, without affecting the operational environment of the ASU.

		RMS Requirement	Not-filtered	Filtered
Drag-free point acceleration with control with 2 DFS [nm/s²]	X	4	4.8	1.1
	Y	4	5.0	1.5
	Z	4	5.0	1.6
Drag-free point acceleration with control with 1 DFS [nm/s²]	X	4	5.0	1.3
	Y	4	8.8	3.8
	Z	4	8.9	4.10
SC angular acceleration [nrad/s²]	X	no	26.3	21.6
	Y	8	14.4	4.4
	Z	8	14.3	4.0
SC angular rate [nrad/s]	X	330	250	249
	Y	14.5	19.3	18.7
	Z	14.5	18.8	17.6

Table 4: Drag-free and attitude control simulation results.

It should be noted that simulation results of (III) demonstrated that the drag-free control is possible with only one drag-free sensor in combination with a gravity gradient model to place the drag-free point. This gives a potential for either mass savings or redundancy.

The statistical analysis of the PST measurements revealed the fact that the Gaussian distribution of the PST measurements is preserved as long as the guide star spot always remains in the same CCD pixel. This is due to the fact that the PST centroiding error, the main contributor of the PST measurement errors, is linear over 1 pixel, but jumps between pixels (non-linearity). The results of the statistical analysis when the guide star is centered within one pixel is shown in Fig 12. In comparison to this Fig 13 shows the results of the analysis when the guide star is centered within four pixels, i.e. at the edges of the pixels. The results are superimposed with the normal Gaussian distribution.

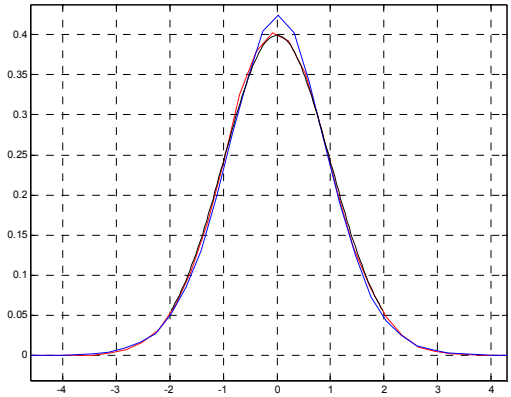

Fig 12: Statistical analysis of PST measurements (guide star centered within 1 pixel)

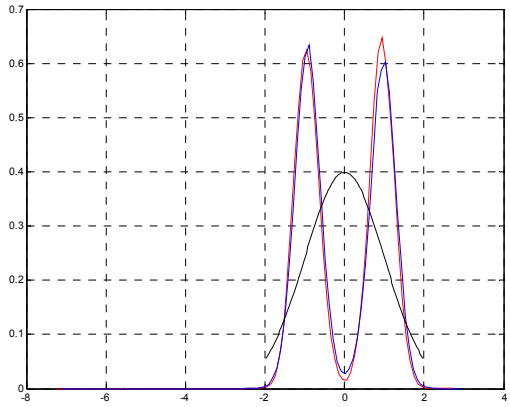

Fig 13: Statistical analysis of PST measurement (guide star centered within 4 pixels)

From the results of the robustness analysis it can be seen that the control system is insensitive to parameter uncertainties such as:

- ±10% uncertainty in mass properties, including products of inertia
- 10 % thruster mismatch, which leads to coupling between linear and angular motion
- environment disturbances and spacecraft magnetic dipole directions
- variation of the distance between spacecraft CoM and drag-free point (5 – 10 cm)
- maximum PST centroiding error

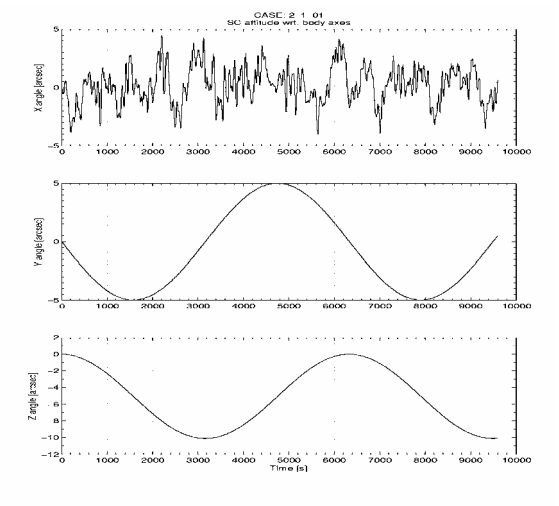

Fig 14: SC attitude on X, Y and Z axes [arcsec]

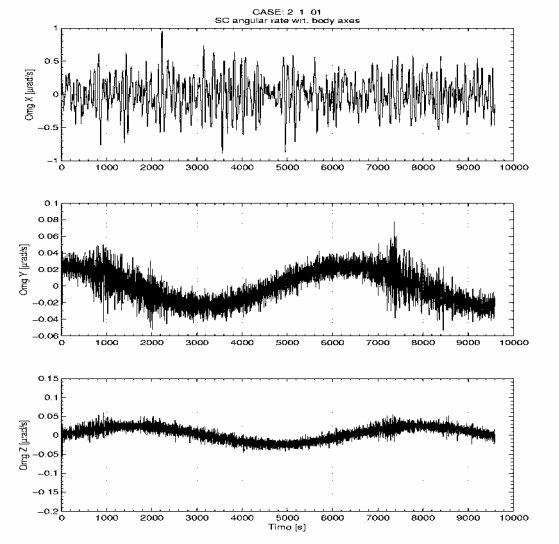

Fig 15: SC rate on X, Y and Z axes [µrad/s]

The simulation results on the PST acquisition performance (type (I)) show that with initial conditions of 1 arcsec/s and 15 arcsec in rate and attitude on all spacecraft axes, the transition to the initial DFACS mode converged successfully in all cases. The initial rate is a factor of 5 larger than typical steady state rates of a conventional attitude control mode based on a 3-axis star tracker. In the context of PST acquisition it should be kept in mind that the PST's field of view is designed to be ±25 arcsec. The trajectory of a typical acquisition sequence can be seen in Fig 16.

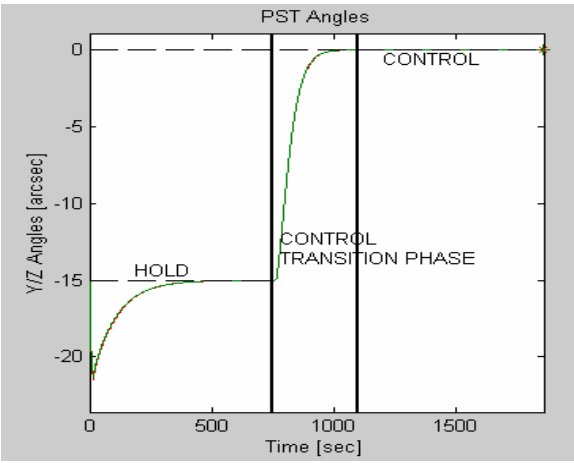

Fig 16: Trajectory of a typical acquisition sequence

The alternative attitude approach using additional angular acceleration information was not studied in detail since the results of the simulation campaign clearly showed that the attitude control for the transverse axes (y and z) can be implemented based on PST attitude information only.

CRITICAL TECHNOLOGY DEVELOPMENT

Two DFACS specific components are most demanding from a technological point of view: the drag-free sensor and the micro-propulsion system. Over the course of the study these two components have been studied in detail and possible solutions have been reviewed.

The PST is a part of the payload and not a "pure" DFACS component. Its design is very challenging and reported in reference [3, 5].

Drag-Free Sensor

The Drag-Free Sensor (DFS) study concluded that the GRADIO sensor to be flown on GOCE could meet the required sensor performance for HYPER. However the study also showed that one item that remains critical is the (constant) sensor bias which is in the order of 10^{-5} m/s^2 in the less-sensitive axis.

The simulations have shown that drag-free control with a bias of 10^{-5} m/s^2 is not feasible, since thruster saturation "weakens" the attitude control in the Y and Z axes. The constant bias part must be improved in order to minimize the maximum thrust demand. An improvement of the bias to a value of 10^{-7} m/s^2 seems feasible technologically (it is limited by the gold wire necessary for the test mass discharging). From a control point of view it adds another 50 μN force demand per thruster (but only in one axis).

Optionally, in order to avoid additional force demand (maximum thrust), low frequency acceleration biases can be "filtered out" in the closed loop control system. This means that low frequencies will not be controlled by drag-free control, but by the ASU phase correction mechanism. However, this leads to an initialisation problem of the drag-free control filters and long transients.

Micro-propulsion

Both, Indium and Caesium FEEPs can be applied for the HYPER mission considering the specifications of these systems. Only minor modifications with respect to the ongoing developments are identified, such as different thruster arrangement and slight increase of thruster actuation frequency. However, this is not considered to be an issue.

In order to assess the performance results rather than dealing with specifications, lifetime tests and qualification programs of the FEEP options have to be monitored at suitable intervals.

CONCULSION

In this paper a drag-free and attitude control system for frame dragging measurements using cold atom interferometers was presented. The required performance of the control system as well as the expected disturbance forces and torques were discussed. In addition Sensor and actuator configurations were evaluated and the derivation and analysis of the control system was presented. The approach in this paper was to use simple, decoupled SISO controllers based on modern optimal control theory. The feasibility of the approach was verified through a comprehensive simulation campaign. Additional findings of the study can be summarized as follows:

- The transition from primary to secondary AOCS was successfully demonstrated for initial conditions of 1 arcsec/s and 15 arcsec.
- Attitude control can be implemented based on PST measurements only, i.e. additional measurements from the DFS are not needed.
- Simulations showed that drag-free control is possible with only one DFS. This gives a potential for either mass savings or redundancy.
- The orbital motion creates an "inertial" rate that exceeds the requirement specification. The latter has to be adapted in the future. This change of the operational envelope should have no impact on the ASU function and performance.
- The control system is insensitive to parameter uncertainties.
- The most critical item that has been identified is the constant DFS bias. Measures have to be taken to reduce the bias to about 10^{-7} m/s^2.

ACKNOWLEDGEMENT

This work was performed under the "HYPER Industrial Feasibility Study", ESTEC Contract Number 16244/02/NL/VD. The authors would like to acknowledge the contributions of Dr. Ernst Maria Rasel, Dr. Philippe Bouyer, and Dr. Arnaud Landragin, who formed the core of the science team. Special thanks go also to Giovanni Cherubini and Simone Becucci from Galileo Avionica, who provided all inputs concerning the precision star tracker.

REFERENCES

[1] Novara, M, Reinhard, R., "HYPER: Hyper Precision Cold Atom Interferometry in Space", Report of the Concurrent Design Facility session at ESA/ESTEC, *ESA document number CDF-09*, September 2000.

[2] Fichter, W., Johann, U., Bagnasco, G., Airey, P., "Spacecraft Design for Atom Interferometry in Space", *Proceedings of the 54th International Astronautical Congress,* September 29 - October 3, 2003, Bremen, Germany.

[3] Airey, S.P., Bagnasco, G., Barilli, M., Becucci, S., Cherubini, G., Romoli, A., "Extreme Accuracy Start Tracker in Support of HYPER Precision Cold Atom Interferometry", American Astronautical Society, Paper AAS 03-505, 2003.

[4] Scheithauer, S., Schleicher, A., Theil, S., "Overview on High Accuracy Acceleration Sensors for Scientific Space Missions", *Proceedings of the 54th International Astronautical Congress,* September 29 - October 3, 2003, Bremen, Germany.

[5] Technical Documentation of the HYPER Industrial Feasibility Study
See ESA/ESTEC web page of HYPER
http://sci.esa.int/science-e/www/area/index.cfm?fareaid=46